One-step Synthesis of Fe-Doped Metal-Organic Framework Nanozymes for Colorimetric Detection and Removal of Tetracycline Antibiotics

Mengru Shan[a], Yufeng Zhang[a], Haobin Jin[a], Siyu Luo[a], Yanqing Cong[a], Shiwen Lv[a], Jing Xu[b] and Yi Zhang[a,*]

[a]Zhejiang Key Laboratory of Solid Waste Pollution Control and Resource Utilization, School of Environmental Science and Engineering, Zhejiang Gongshang University, Hangzhou 310018, China

[b]School of Statistics and Mathematics, Zhejiang Gongshang University, Hangzhou 310018, China

Text

Text S1 Chemicals and reagents

$Co(NO_3)_2·6H_2O$, $Fe(NO_3)_3·9H_2O$, $Cu(NO_3)_2·3H_2O$, $Ce(NO_3)_2·8H_2O$, $Zn(NO_3)_2·6H_2O$, $Ni(NO_3)_2·6H_2O$, Tetracycline (TC), Oxytetracycline (OTC), Doxycycline (DOX), Doxycycline hydrochloride (DHC), Glucose (Glu) , Histidine (His), Erythromycin, sulfamethoxazole (SMX), amoxicillin (AMX), ammonium oxalate, p-benzoquinone (PBQ), tert butanol (TBA), acetic acid, 3,3',5,5'-tetramethylbenzidine (TMB), Nfion perfluorinated resin solution (Nafion), Methanol, Ethanol and Isopropyl alcohol were provided from Shanghai McLean. 2-methylimidazole (2-MIM) and Dimethyl sulfoxide (DMSO) were purchased from Aladdin, Shanghai. Sinopharm Chemical Reagent Co., Ltd provided Bisphenol A (BPA)，Potassium chloride (KCl), Magnesium chloride hexahydrate ($MgCl_2·6H_2O$), Sodium chloride (NaCl), Sodium acetate anhydrous and Calcium chloride ($CaCl_2$). Carbon cloth was purchased from Nantong senyou Carbon Fiber Co., Ltd. Hangzhou Jingong Special Gas Co., Ltd provided O_2 (99.99%) and N_2 (99.99%). All the chemicals were used without further purification. All chemical reagents are analytical grade.

Text S2 The optimal preparation conditions and optimal detection conditions

All absorbance measurements conducted to determine the optimal preparation conditions and optimal detection conditions were performed under the following conditions: ZIF-67/Fe-6 (2 mg/mL, 50 μL), TC (80 mg/L, 100 μL), H_2O_2 (0.04 M, 50 μL), TMB (0.02 M, 50 μL), sodium acetate-acetic acid buffer (0.2 M, pH 4.0, 3750 μL). The mixture was incubated for 10 minutes for color development, and absorbance was measured at 652 nm using a UV-Vis spectrophotometer. Three sets of parallel experiments are conducted on one data point and the average value, standard deviation and relative standard deviation are calculated through eq. S 1, 2 and 3.

$$\bar{x} = \frac{1}{n}\sum_{i=1}^{n} x_i \quad \text{(S1)}$$

To whom correspondence should be addressed. E-mail: zhangyi@zjgsu.edu.cn

$$S = \sqrt{\frac{1}{n-1}\sum_{i=1}^{n}\left(x_i - \bar{x}\right)^2} \quad \text{(S2)}$$

$$RSD\ (\%) = \frac{S}{\bar{x}} \times 100\% \quad \text{(S3)}$$

Where n and i represent the number of parallel groups and the number of data, x_i is the sum of the data, $\bar{x}$ is the average value of the data, S is the standard deviation and RSD is relative standard deviation.

Text S3 Apparatus and characterization

The morphology of the catalyst was characterized by scanning electron microscopy (SEM, EISS Sigma 360). The distribution and proportion of elements on the catalyst were characterized by using secondary electron detector and energy dispersive X-ray spectrometer (EDS, Oxford Xplore 50). The phase structure was characterized by X-ray diffractometer (XRD, Rigaku SmartLab SE). X-ray photoelectron spectroscopy (XPS) was collected on Thermo Scientific K-Alpha. Use electron paramagnetic resonance (EPR，Bruker EMXPlus) spectrometer to identify free radicals. The Zeta potential was tested by the UK-based Malvern Zetasizer Pro.

The electrochemical performance of ZIF-67/Fe-6 was analyzed by CHI660E electrochemical workstation. In the three-electrode system at 0.2 M NaAc-HAc buffer solution (pH = 4.0), 1 × 1 cm^2 ZIF-67/Fe-6, platinum plate, and Silver/Silver Chloride electrode (Ag/AgCl) are used as working electrodes, counter electrodes, and reference electrodes, respectively. First, prepare the ZIF-67/Fe-6 electrode (1×1 cm^2) using carbon paper and Nafion solution. Ultrasonic the Nafion (1%) mixture containing 10 mg of ZIF-67/Fe-6 for 5 minutes. Then, take 20 μL of the mixture each time and drop-coat it on the carbon paper three times, followed by natural airdrying. In addition, the ZIF-67-3, ZIF-67-6, and ZIF-67/Fe-3 electrodes were all prepared in the same way, except that 10 mg of ZIF-67/Fe-6 was replaced with 10 mg of ZIF-67-3, ZIF-67-6, and ZIF-67/Fe-3 respectively. Linear sweep voltammetry (LSV), cyclic voltammetry (CV), and Tafel measurements are all conducted in 100 mL of NaAc-HAc buffer solution (0.2 M, pH = 4.0). Electrochemical Impedance Spectroscopy (EIS) is tested in 100 ml of an electrolyte composed of 0.165 g of potassium ferricyanide, 0.211 g of potassium

ferrocyanide, and 0.7455 g of potassium chloride. The impedance of different electrodes is also tested in a three electrode system.

Text S4 DFT

We used the DFT as implemented in the CP2K 2024.3 in all calculations. The exchange-correlation potential is described by using Grimme's DFT-D3 with (Beck-Johnson)BJ factormodified generalized gradient approximation of Perdew-Burke-Ernzerhof (GGA-PBE-D3(BJ)) during all calculations. During DFT calculations, The convergence criteria of 1.0 E-06 for electron step, max atomic force of 4.5 E-4, max geometry change of 3 E-3 were set to ensure that structures are fully optimized and the electron wave function had converged to a stable state so that the energyof the system could remain stable.[1-4] The DZVP-MOLOPT-SR-GTH basis set was used during geometry optimization & vibrational frequencies, and TZV2P-MOLOPT-SR-GTH basis set during single point calculations. All wavefunction analysis was carried out on Multiwfn 3.8 Dev.[5, 6] The opted structures and charge density difference plots are visualized by VESTA.[7]

Text S5 Detection of TCs in actual samples

The lake water was collected from Mohu Lake of Zhejiang Gongshang University, and the river water was collected from the inland river of Qiantang River in Qiantang District. Spiked into actual water samples to prepare TCs at different concentrations.

Text S6 The removal of TCs

In the experiment of degrading TCs, the concentrations of H_2O_2 and the catalyst are kept the same as those in the detection system. The concentration of TCs is uniformly 2 mg/L, and the content of TCs is detected by by high performance liquid chromatography (HPLC). The separation was carried out on a C18 chromatographic column (4.6 mm × 250 mm, 5 μm). The mobile phase consisted of methanol and 0.01 M aqueous oxalic acid solution with a volume ratio of 47:53. The flow rate was set at 1.0 mL/min, and the detection wavelength was 355 nm. The column temperature was maintained at 30 °C, and the injection volume was 20 μL.[8]

Removal percent (%) = $(1 - C_t / C_0) \times 100\%$

where, C_0 and C_t represent the concentrations (mg/L) of TCs of initial and time-

dependent after both adsorption and degradation, respectively.

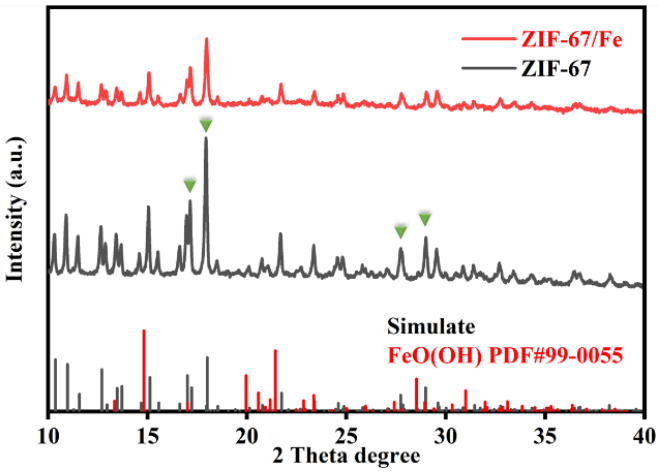

Fig. S1 XRD patterns of ZIF-67 and ZIF-67/Fe-6.

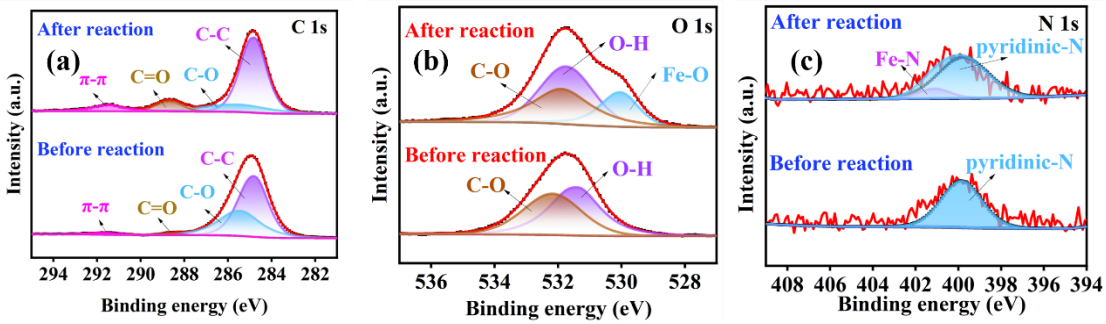

Fig. S2 (a) The C 1s XPS spectrum of ZIF-67/Fe-6. (b) The O 1s XPS spectrum of ZIF-67/Fe-6. (c) The N 1s XPS spectrum of ZIF-67/Fe-6.

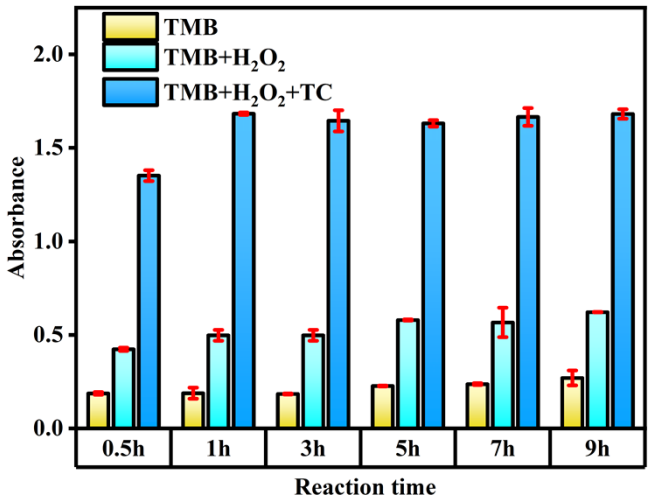

Fig. S3 Different preparation time of ZIF-67/Fe-6. Experimental conditions: ZIF-67/Fe-6: 2 mg/mL^{-1}, TMB: 0.25 mM, H_2O_2: 0.5 mM, TC: 2 mg/L.

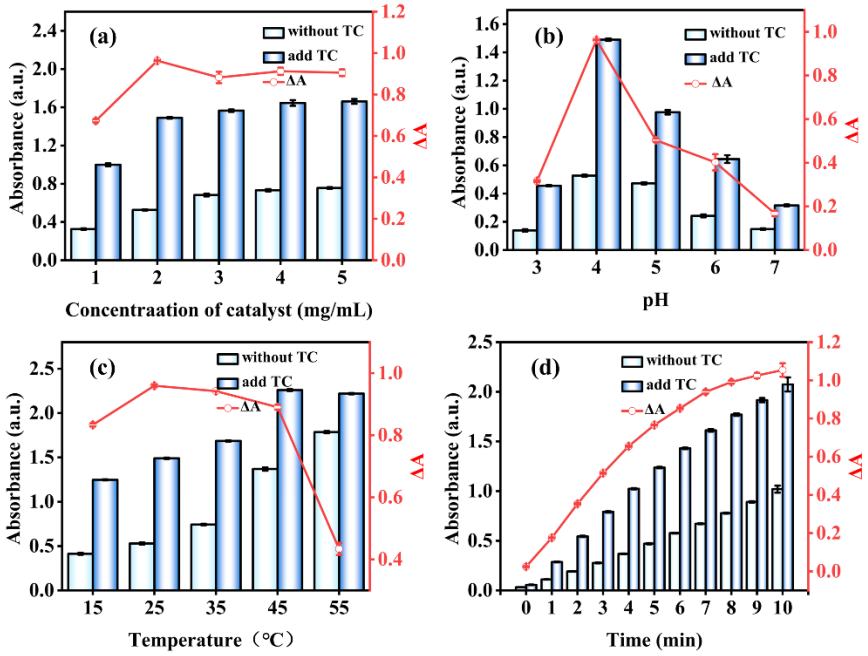

Fig. S4 The optimal reaction conditions for ZIF-67/Fe-6. (a) The concentration of ZIF-67/Fe-6. (b) The pH of sodium acetate-acetic acid buffer solution. (c) The temperature of the reaction system. (d) The concentration of TMB and H_2O_2.

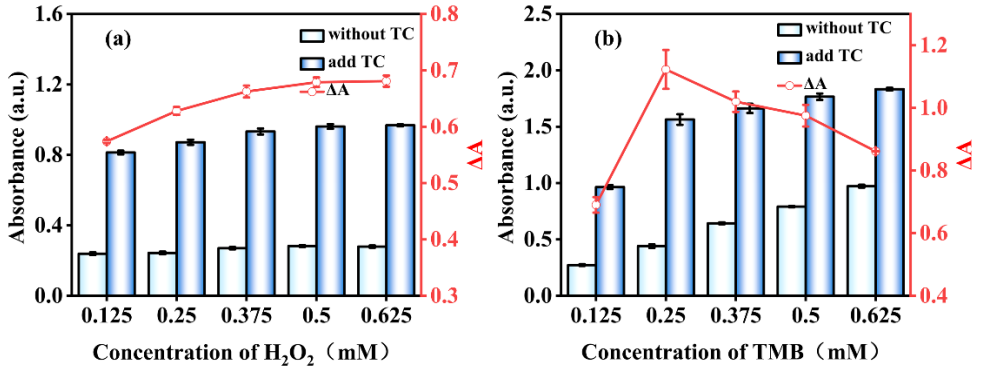

Fig. S5 Selection of optimal concentrations for H_2O_2 and TMB. (a) H_2O_2. (b) TMB.

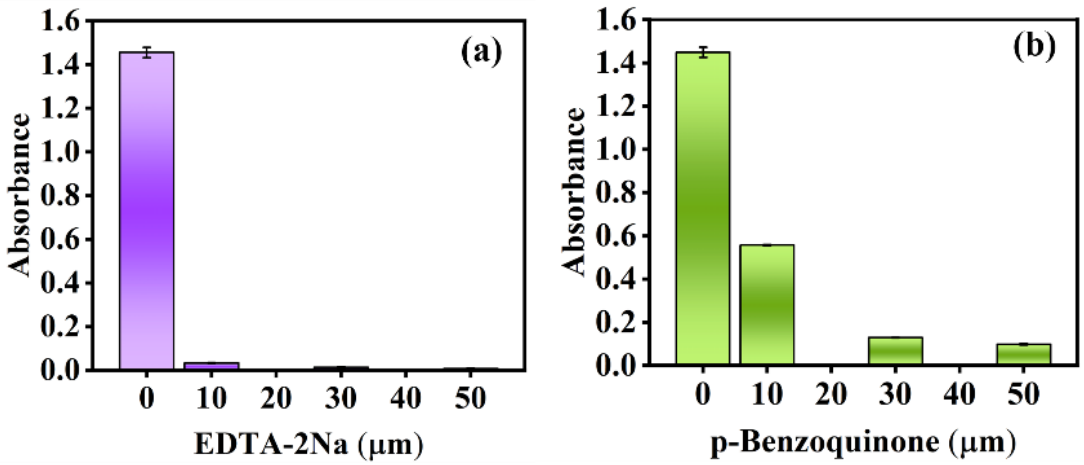

Fig. S6 The inhibitory effect of free-radical scavengers at different concentration gradients on the absorbance at 652 nm. (a) EDTA-2Na. (b) p-Benzoquinone.

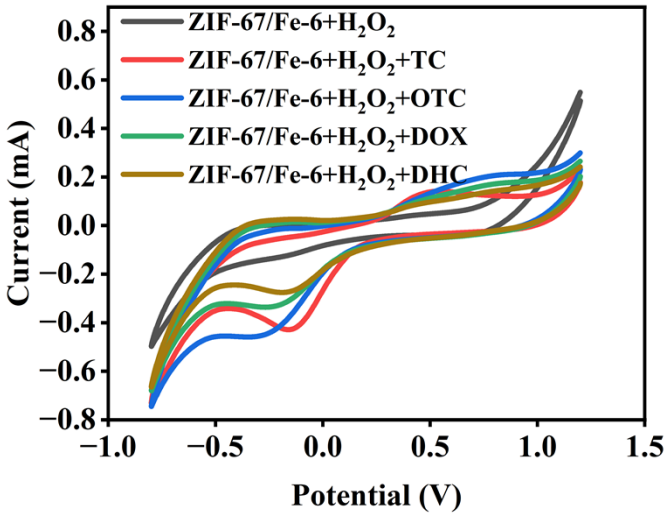

Fig. S7 Cyclic voltammograms between ZIF-67/Fe-6 and tetracyclines (TC, OTC, DOX and DHC).

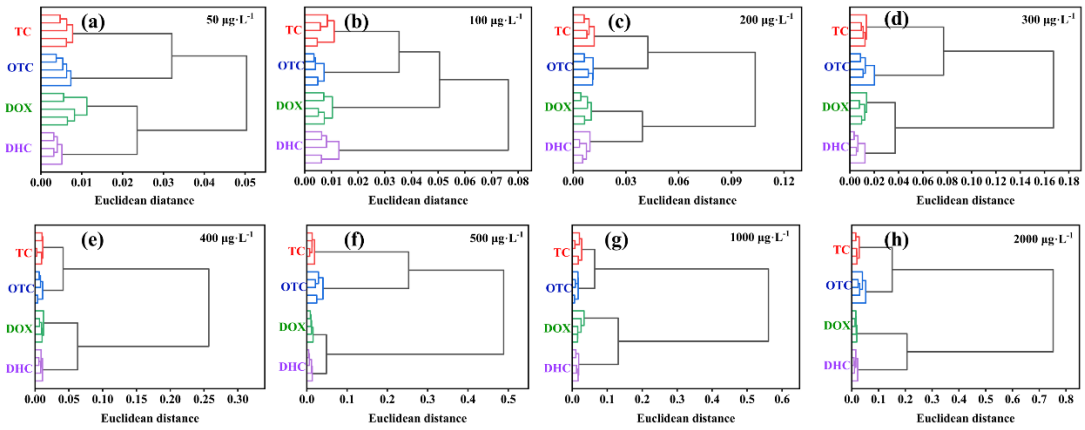

Fig. S8 Hierarchical Clustering Analysis of TCs at Various Concentrations.

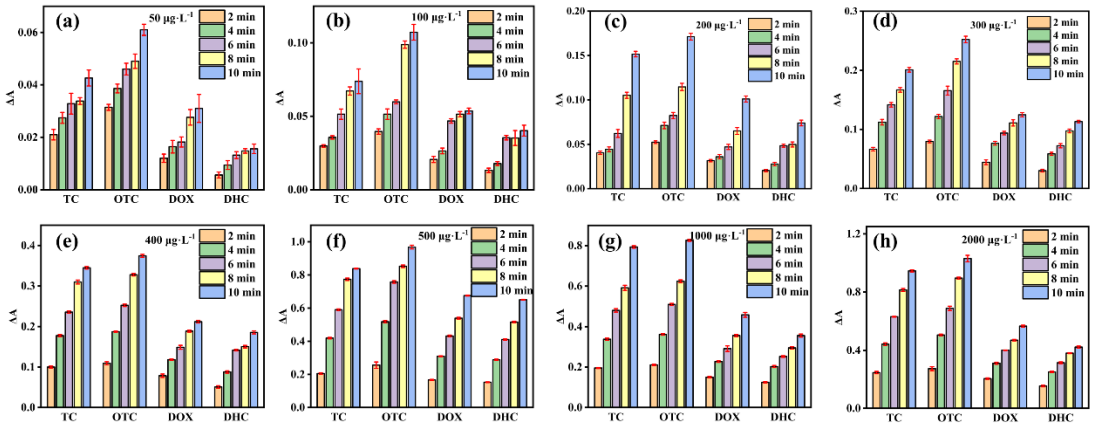

Fig. S9 Fingerprint Profiles of TCs at Different Concentrations.

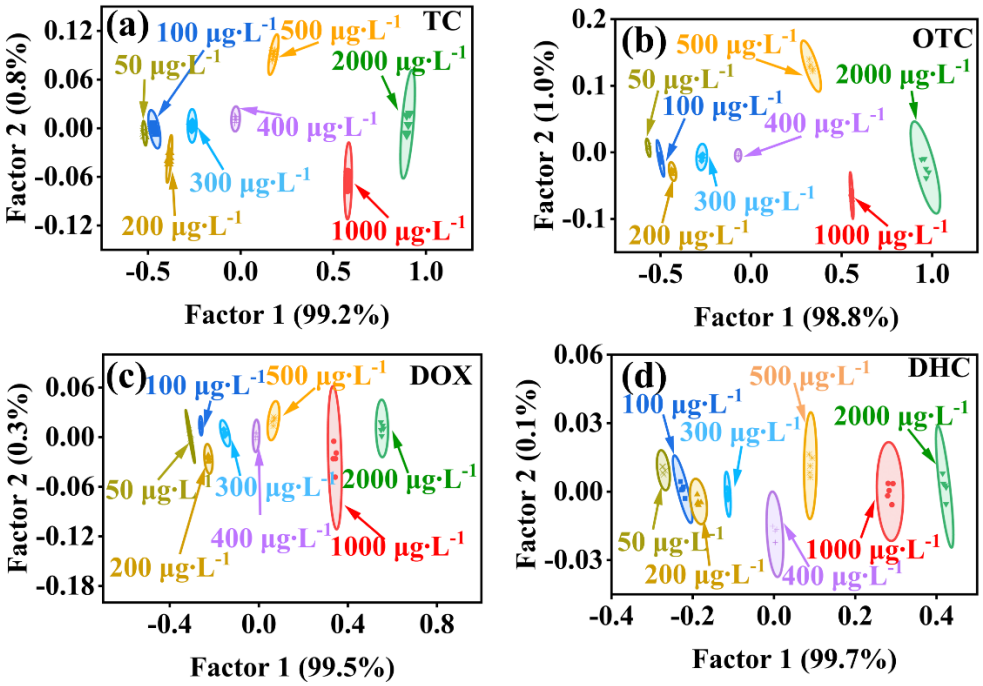

Fig. S10. LDA plots of TCs at various concentrations: (a), OTC (b), DOX (c) and DHC (d).

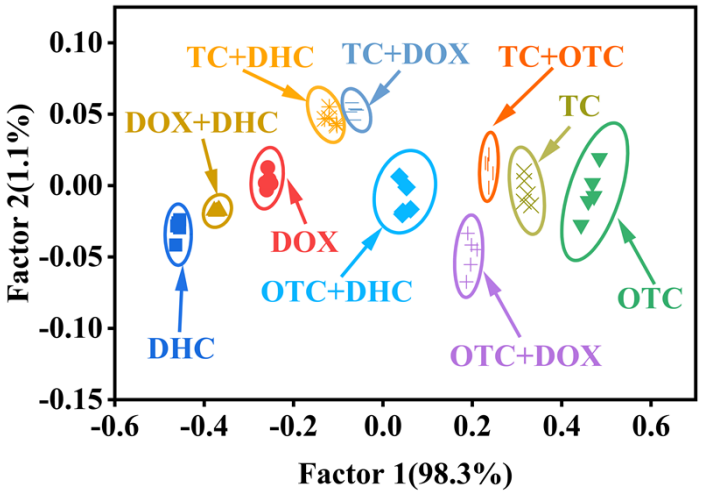

Fig. S11 LDA plot of the equimolar mixture of four TCs.

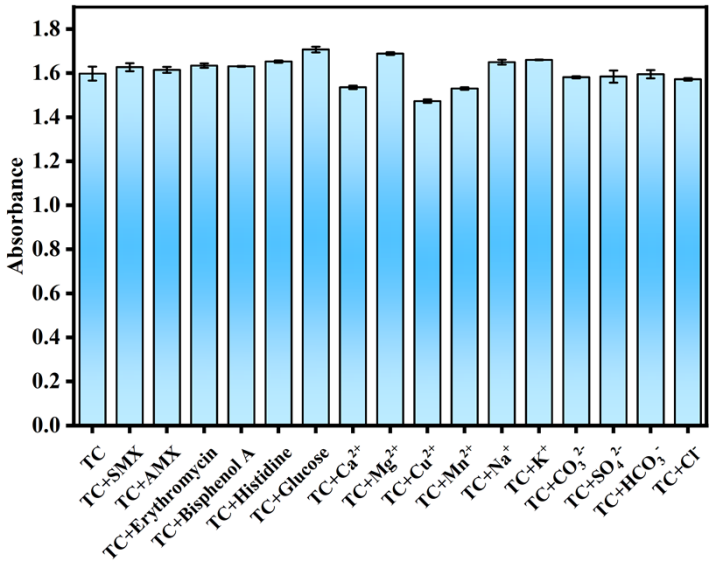

Fig. S12 The interference effects of other antibiotics, phenolic compounds, metal salts, and inorganic anions on the detection of TC.

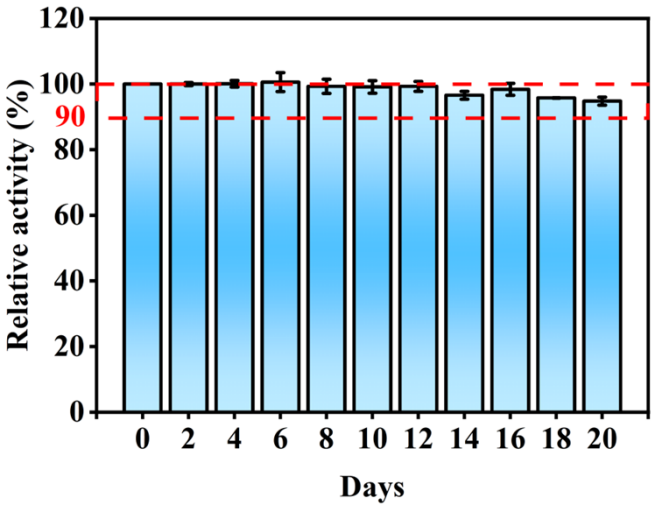

Fig. S13 ZIF-67/Fe-6 20-Day stability assay.

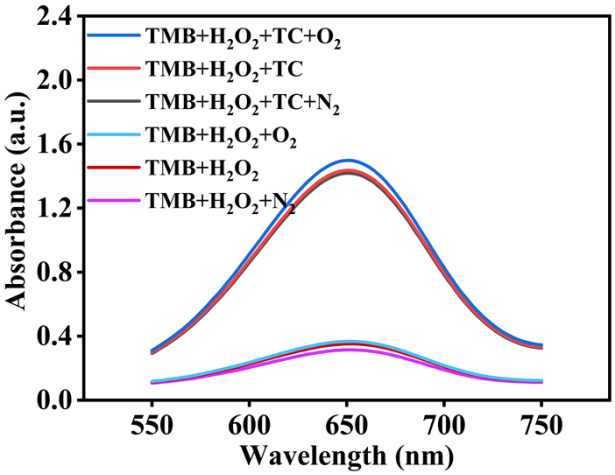

Fig. S14 Effect of Nitrogen (N_2) and Oxygen (O_2) on Absorbance.

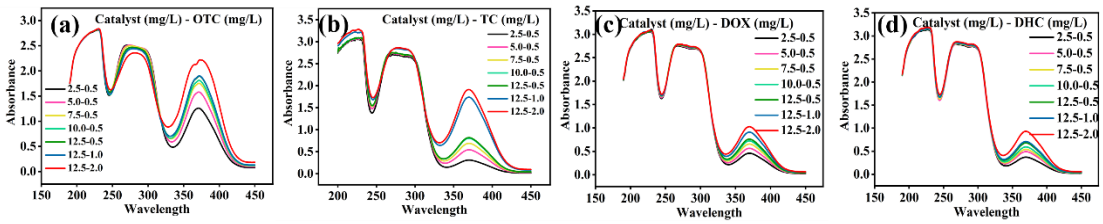

Fig. S15 UV-vis absorption spectra of ZIF-67/Fe-6 and TCs at different mass concentration ratios (ZIF-67/Fe-6 : TCs, mg/L): 2.5 : 0.5, 5.0 : 0.5, 7.5 : 0.5, 10.0 : 0.5, 12.5 : 0.5, 12.5 : 1.0, 12.5 : 2.0. (a) OTC. (b) TC. (c) DOX. (d) DHC.

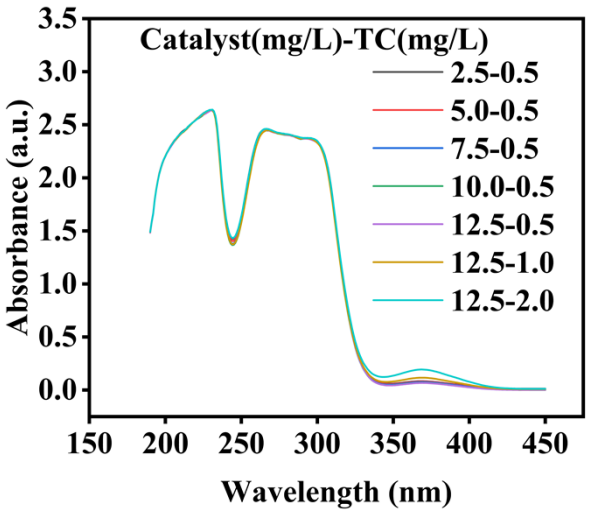

Fig. S16 UV-vis absorption spectra of ZIF-67 and TC at different mass concentration ratios (ZIF-67 : TC, mg/L): 2.5 : 0.5, 5.0 : 0.5, 7.5 : 0.5, 10.0 : 0.5, 12.5 : 0.5, 12.5 : 1.0, 12.5 : 2.0.

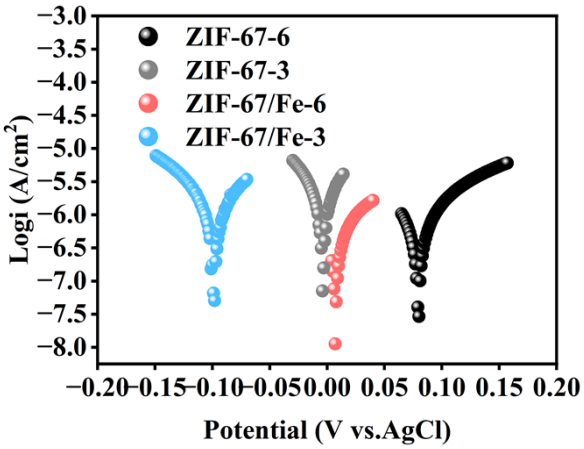

Fig. S17 Tafel polarization curves of ZIF-67-6, ZIF-67-3, ZIF-67/Fe-6 and ZIF-67/Fe-3.

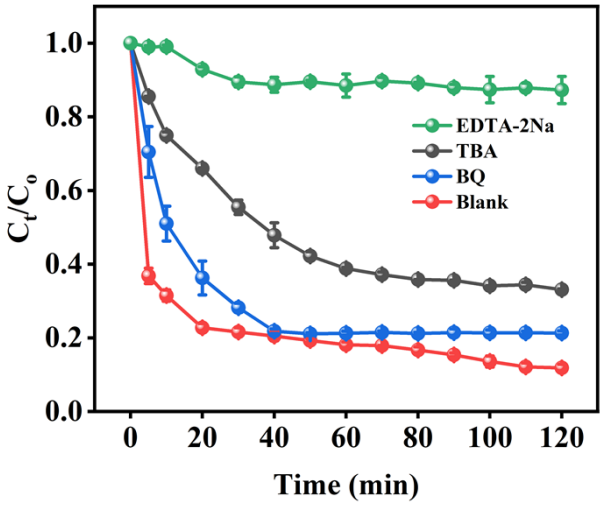

Fig. S18 Capture agent experiments for TC degradation by ZIF-67/Fe-3.

Table S1: Comparison of the enzymatic kinetic parameters

Materials	TMB		H_2O_2		Ref.
	K_m (mM)	Vmax (10^{-8} M/s)	K_m (mM)	Vmax (10^{-8} M/s)	
ZIF-67/Fe-6	0.839	1.942	0.109	3.87	This work
ZIF-67/Fe-3	1.142	1.891	0.174	3.71	This work
HRP	0.43	10.0	3.7	8.71	[9]
Fe_3O_4 MNPs	154	9.78	0.098	3.44	[9]
Co_3O_4@Co-Fe oxide DSNCs	0.48	5.32	0.24	5.18	[10]
Co-Fe oxide	0.54	4.07	0.33	3.56	[10]
Co_3O_4 SSNCs	1.09	2.66	0.80	2.33	[10]
NH_2–MIL–88B	0.605	8.547	0.169	1.786	[11]
ZIF-67	13.69	0.35	3.52	0.28	[12]
Fe-MOF-GOx	2.60	5.60	1.30	2.50	[13]
Fe-Ce-MOL	0.386	24.4	0.588	19.2	[14]
Fe_3O_4-Fe^0/Fe_3C	0.88	54.67	1.46	5.67	[15]

Table S2: Detection limit comparison

Materials	Analyte	Method	Time (min)	Linear range (μg/L)	LOD (μg/L)	Ref.
ZIF-67/Fe	OTC	Colorimetric	10	50-1000	17.78	this
	TC	Colorimetric	10	50-1000	19.71	work
	DOX	Colorimetric	10	50-1000	33.39	
	DHC	Colorimetric	10	50-1000	38.05	
UiO-66(Zr)	TC	Colorimetric	2	88-8880	62.1	[16]
NH_2-MIL-88(B)	TC	Colorimetric	30	22.2-444	20.42	[11]
α-Fe_2O_3 QDs/TS-1	OTC	Colorimetric	20	10-10000	19.7	[17]
	DOX	Colorimetric	20	0-500	23.1	
	TC	Colorimetric	20	500-10000	35.9	
MnO_2/ZnNC	TC	Colorimetric	30	444-88800	99.54	[18]
	DOX	Colorimetric	30	444-88800	198.73	
Fe_3O_4 nanozyme	TC	Colorimetric	30	44.4-444	19.98	[19]
	OTC	Colorimetric	30	22.2-444	11.54	
	DOX	Colorimetric	30	22.2-444	21.31	
FL-$Ti_3C_2T_x$	TC	Colorimetric	30	341-136574	27	[20]
Fe/Co-MOF	TC	Colorimetric	15	350-220000	71.9	[21]
MIL-101(Fe)	TC	Colorimetric	50	444-3552	1105.5	[22]
NH_2-MIL-101(Fe)	TC	Colorimetric	10	200-40000	66.6	[23]

Table S3: Determinations of TCs in real samples by Colorimetry and HPLC

Samples	Analyte	Spiked (μg/L)	Colorimetry			HPLC
			Detected (μg/L)	Recovery (%)	RSD (%)	Detected (μg/L)
Lake water	TC	50	48.55±3.52	97.10	7.25	48.33±0.31
Lake water	TC	100	102.05±2.07	102.04	2.03	102.16±0.93
Lake water	TC	200	192.89±2.23	96.44	1.15	195.86±0.53
River water	TC	50	54.82±1.7	109.63	3.10	51.8±0.45
River water	TC	100	102.29±4.48	102.28	4.38	100.8±0.33
River water	TC	200	205.18±2.99	102.59	1.45	202.13±0.94
Lake water	OTC	50	48.02±1.81	96.04	3.77	49.46±0.58
Lake water	OTC	100	100.86±2.82	100.86	2.79	101.8±0.24
Lake water	OTC	200	198.15±1.44	99.07	0.72	201.36±0.82
River water	OTC	50	54.44±2.29	108.8	4.20	51.5±0.43
River water	OTC	100	102.35±1.98	102.34	1.93	100.16±0.81
River water	OTC	200	199.63±3.22	99.81	1.61	198.03±1.27
Lake water	DOX	50	46.33±2.38	92.65	5.13	49.33±0.31
Lake water	DOX	100	103.06±3.79	103.06	3.67	101.43±0.63
Lake water	DOX	200	195.31±5.07	97.65	2.59	201.36±0.86
River water	DOX	50	48.78±2.89	97.55	5.91	49.5±0.54
River water	DOX	100	105.92±3.65	105.91	3.44	100.83±0.76
River water	DOX	200	200.61±2.77	100.30	1.37	200.2±0.93
Lake water	DHC	50	47.44±2.37	94.88	4.99	49.46±0.84
Lake water	DHC	100	105.58±2.37	105.58	2.24	101.8±0.64
Lake water	DHC	200	208.37±2.37	104.18	1.13	202.43±0.46
River water	DHC	50	52.56±2.37	105.11	4.51	50.73±0.49
River water	DHC	100	101.86±3.09	101.86	3.02	99.8±0.54
River water	DHC	200	212.56±3.15	106.27	1.48	201.5±0.99

References

1. , <Matthias Ernzerhof. Generalized Gradient Approximation Made Simple.pdf>.
2. M. Ernzerhof and G. E. Scuseria, Assessment of the Perdew–Burke–Ernzerhof exchange-correlation functional, *The Journal of Chemical Physics*, 1999, **110**, 5029-5036.
3. S. Grimme, J. Antony, S. Ehrlich and H. Krieg, A consistent and accurateab initioparametrization of density functional dispersion correction (DFT-D) for the 94 elements H-Pu, *The Journal of Chemical Physics*, 2010, **132**.
4. S. Grimme, S. Ehrlich and L. Goerigk, Effect of the damping function in dispersion corrected density functional theory, *J. Comput. Chem.*, 2011, **32**, 1456-1465.
5. T. Lu and F. Chen, Multiwfn: A multifunctional wavefunction analyzer, *J. Comput. Chem.*, 2012, **33**, 580-592.
6. T. Lu, A comprehensive electron wavefunction analysis toolbox for chemists, Multiwfn, *The Journal of Chemical Physics*, 2024, **161**.
7. K. Momma and F. Izumi, VESTA 3 for three-dimensional visualization of crystal, volumetric and morphology data, *J. Appl. Crystallogr.*, 2011, **44**, 1272-1276.
8. L. Liu, C. Han, G. Ding, M. Yu, Y. Li, S. Liu, Y. Xie and J. Liu, Oxygen vacancies-enriched Cu/Co bimetallic oxides catalysts for high-efficiency peroxymonosulfate activation to degrade TC: Insight into the increase of Cu+ triggered by Co doping, *Chem. Eng. J.*, 2022, **450**, 138302.
9. L. Gao, J. Zhuang, L. Nie, J. Zhang, Y. Zhang, N. Gu, T. Wang, J. Feng, D. Yang, S. Perrett and X. Yan, Intrinsic peroxidase-like activity of ferromagnetic nanoparticles, *Nature Nanotechnology*, 2007, **2**, 577-583.
10. Q. Chen, X. Zhang, S. Li, J. Tan, C. Xu and Y. Huang, MOF-derived Co3O4@Co-Fe oxide double-shelled nanocages as multi-functional specific peroxidase-like nanozyme catalysts for chemo/biosensing and dye degradation, *Chem. Eng. J.*, 2020, **395**, 125130.
11. Z. Li, F. Meng, R. Li, Y. Fang, Y. Cui, Y. Qin and M. Zhang, Amino-functionalized Fe(III)-Based MOF for the high-efficiency extraction and ultrasensitive colorimetric detection of tetracycline, *Biosens. Bioelectron.*, 2023, **234**, 115294.
12. S. Wang, D. Xu, L. Ma, J. Qiu, X. Wang, Q. Dong, Q. Zhang, J. Pan and Q. Liu, Ultrathin ZIF-67 nanosheets as a colorimetric biosensing platform for peroxidase-like catalysis, *Analytical and Bioanalytical Chemistry*, 2018, **410**, 7145-7152.
13. W. Xu, L. Jiao, H. Yan, Y. Wu, L. Chen, W. Gu, D. Du, Y. Lin and C. Zhu, Glucose Oxidase-Integrated Metal–Organic Framework Hybrids as Biomimetic Cascade Nanozymes for Ultrasensitive Glucose Biosensing, *ACS Applied Materials & Interfaces*, 2019, **11**, 22096-22101.
14. L. Chen, K. Yang, C. Wang, D. Han and J. Wen, Next-generation of a Fe-Ce double variable-valence metals modulated high-efficiency nanozyme, *Chemical Engineering Journal*, 2024, **495**, 153314.
15. A. F. Baye, H. Thi Nguyen and H. Kim, Fe0/Fe3C-assisted Fe3O4 redox sites as robust peroxidase mimics for colorimetric detection of H2O2, *Sensors and Actuators B: Chemical*, 2023, **377**, 133097.
16. C. Shi, S. Pu, L. Wu and X. Hou, A “turn on” colorimetric system based on bimetallic UiO-66(Zr/Ce) for rapid sensing of tetracyclines through visible light triggering, *Sensors and Actuators B: Chemical*, 2023, **379**.
17. F. Meng, K. Wei, Y. Li, L. Zhang, S. Xu, X. Shi and B. Tang, Efficient synthesis of

multifunctional α-Fe2O3 QDs/TS-1 as an artificial nanozyme for simultaneous colorimetric detection and photodegradation of tetracyclines, *Chem. Eng. J.*, 2024, **498**.

18. X. Li, L. Jiang, T. R. Ahmad, J. Jin, J. Chen and X. Yang, Innovative dual-oxidase nanozyme sensor array for rapid detection of tetracyclines in animal-derived foods, *J. Hazard. Mater.*, 2026, **503**, 141213.
19. Y. Wang, Y. Sun, H. Dai, P. Ni, S. Jiang, W. Lu, Z. Li and Z. Li, A colorimetric biosensor using Fe_3O_4 nanoparticles for highly sensitive and selective detection of tetracyclines, *Sens. Actuators B Chem.*, 2016, **236**, 621-626.
20. W. Wang, Y. Yin and S. Gunasekaran, Nanozymatic degradation and simultaneous colorimetric detection of tetracycline, *Food Chem.*, 2023, **426**, 136607.
21. X. Yue, C. Wu, C. Hao and Y. Bai, Defective Fe/Co-MOF with abundant oxygen vacancies as an efficient oxidase mimic for colourimetric and sensitive determination of tetracycline, *New J. Chem.*, 2024, **48**, 16323-16330.
22. F. Niu, H. Sun, Y. Gao, S. Ding, Q. Xu, X. Dong, X. Wang, X. Zhang, X. Wang and Y. Fang, Killing two birds with one stone: a simple and integrated platform based on an Fe-MOF for dual-mode detection and photocatalytic elimination of tetracycline, *Analyst*, 2025, **150**, 3423-3430.
23. Z. Qin, T. Peng, X. Qin, G. Liu and H. Zhang, Colorimetric/fluorescent dual-mode biosensor based on metalloporphyrin covalently modified NH2-MIL-101(Fe) with highly efficient peroxidase-like activity for the detection of tetracycline in honey samples, *Food Chem.*, 2025, **484**, 144387.